AEDC-TR-81-33

c2

Hypervelocity Impact Instrumentation Development

P. H. Dugger and R. E. Hendrix
ARO, Inc.

November 1981

Final Report for Period October 1, 1978 – September 30, 1979

ARNOLD ENGINEERING DEVELOPMENT CENTER
ARNOLD AIR FORCE STATION, TENNESSEE
AIR FORCE SYSTEMS COMMAND
UNITED STATES AIR FORCE

NOTICES

When U. S. Government drawings, specifications, or other data are used for any purpose other than a definitely related Government procurement operation, the Government thereby incurs no responsibility nor any obligation whatsoever, and the fact that the Government may have formulated, furnished, or in any way supplied the said drawings, specifications, or other data, is not to be regarded by implication or otherwise, or in any manner licensing the holder or any other person or corporation, or conveying any rights or permission to manufacture, use, or sell any patented invention that may in any way be related thereto.

Qualified users may obtain copies of this report from the Defense Technical Information Center.

References to named commercial products in this report are not to be considered in any sense as an endorsement of the product by the United States Air Force or the Government.

This report has been reviewed by the Office of Public Affairs (PA) and is releasable to the National Technical Information Service (NTIS). At NTIS, it will be available to the general public, including foreign nations.

APPROVAL STATEMENT

This report has been reviewed and approved.

Marshall K. Kingery

MARSHALL K. KINGERY
Directorate of Technology
Deputy for Operations

Approved for publication:

FOR THE COMMANDER

Marion L. Laster

MARION L. LASTER
Director of Technology
Deputy for Operations

UNCLASSIFIED

SECURITY CLASSIFICATION OF THIS PAGE *(When Data Entered)*

REPORT DOCUMENTATION PAGE		READ INSTRUCTIONS BEFORE COMPLETING FORM
1. REPORT NUMBER AEDC-TR-81-33	2. GOVT ACCESSION NO.	3. RECIPIENT'S CATALOG NUMBER
4. TITLE *(and Subtitle)* HYPERVELOCITY IMPACT INSTRUMENTATION DEVELOPMENT		5 TYPE OF REPORT & PERIOD COVERED Final Report - October 1, 1978 to September 30, 1979 6 PERFORMING ORG. REPORT NUMBER
7. AUTHOR(s) P. H. Dugger and R. E. Hendrix, ARO, Inc., a Sverdrup Corporation Company		8. CONTRACT OR GRANT NUMBER(s)
9 PERFORMING ORGANIZATION NAME AND ADDRESS Arnold Engineering Development Center Air Force Systems Command Arnold Air Force Station, Tennessee 37389		10. PROGRAM ELEMENT, PROJECT, TASK AREA & WORK UNIT NUMBERS Program Element 64406F
11. CONTROLLING OFFICE NAME AND ADDRESS Arnold Engineering Development Center/DOS Air Force Systems Command Arnold Air Force Station, Tennessee 37389		12. REPORT DATE November 1981 13. NUMBER OF PAGES 27
14. MONITORING AGENCY NAME & ADDRESS(if different from Controlling Office)		15. SECURITY CLASS. *(of this report)* UNCLASSIFIED 15a. DECLASSIFICATION/DOWNGRADING SCHEDULE N/A

16. DISTRIBUTION STATEMENT *(of this Report)*

Approved for public release; distribution unlimited.

17. DISTRIBUTION STATEMENT *(of the abstract entered in Block 20, if different from Report)*

18. SUPPLEMENTARY NOTES

Available in Defense Technical Information Center (DTIC)

19. KEY WORDS *(Continue on reverse side if necessary and identify by block number)*

aeroballistic
hypersonic wind tunnels
hypervelocity impact
high speed photography
sequential photography
lasers
electromagnetic radiation
microwaves
radiometers
spectrometers
screens

20. ABSTRACT *(Continue on reverse side if necessary and identify by block number)*

The instrumentation capabilities of the Arnold Engineering Development Center (AEDC) von Kármán Gas Dynamics Facility's (VKF) aeroballistic ranges have been expanded to facilitate studies of hypervelocity impact-related phenomena. Two instrumentation systems for characterizing clouds of debris resulting from impact have been developed and put to use: (1) An extremely high-speed sequential laser photography system provides photographic data

DD FORM 1 JAN 73 1473 EDITION OF 1 NOV 65 IS OBSOLETE

UNCLASSIFIED

SECURITY CLASSIFICATION OF THIS PAGE *(When Data Entered)*

20. ABSTRACT (Continued)

describing debris cloud growth characteristics at framing rates from 10^4 sec^{-1} to 10^7 sec^{-1}. This system can resolve debris particles as small as 0.001 in. (2) X-ray shadowgraph systems with exposure times of 30 nsec can record debris velocity and mass data and can discern aluminum particles as small as 0.063 in. and steel particles as small as 0.031 in. Electromagnetic radiation generated by hypervelocity impact can be explored in a variety of ways: A high-speed framing camera capable of framing rates as high as 1.4×10^6 sec^{-1} allows studies of the relative intensity, physical extent, and growth and decay rates of impact flashes. Development of microwave radiometers extends the capability for quantitative measurements (down to levels as low as 3×10^{-14} w/sr-μm) of radiation related to hypervelocity impact to include two frequencies in the centimeter-wave region of the electromagnetic spectrum--8.6 and 35 GHz. A time-integrated spectrometer provides data characterizing the impact flash in terms of relative intensity versus wavelength within the spectral band from 3500 to 6800 Å. Special make-screen detection systems provide trigger signals for photographic and radiation measurement instrumentation systems. These detection systems have demonstrated reliabilities of 87 percent for model detection and 79 percent for debris detection.

PREFACE

The work reported herein was conducted by the Arnold Engineering Development Center (AEDC), Air Force Systems Command (AFSC). The results were obtained by ARO, Inc. (a Sverdrup Corporation Company), AEDC Division, operating contractor for the AEDC, AFSC, Arnold Air Force Station, Tennessee. Marshall K. Kingery, Directorate of Technology (DOT), was the Air Force project manager. The research was done under ARO Project Nos. V34L-27 and V42S-20, and the manuscript was submitted for publication on October 2, 1979.

The authors acknowledge the contributions of C. P. Enis, R. C. Hensley, J. W. Hill, W. F. Henderson, L. E. Simpson, and E. D. Tidwell, ARO, Inc., who performed the experimental work of the programs.

Authors P. H. Dugger and R. E. Hendrix, as well as all personnel in the preceding paragraph, with the exception of R. C. Hensley, are currently employed by Calspan Field Services, Inc., AEDC Division. R. C. Hensley is employed by Sverdrup Technology, Inc., AEDC Group.

CONTENTS

ILLUSTRATIONS

Figure

1.0 INTRODUCTION

In recent years requirements for measurement of hypervelocity impact-related phenomena have increased beyond existing capabilities. The aeroballistic ranges of the von Kármán Gas Dynamics Facility (VKF) of the Arnold Engineering Development Center (AEDC) are used routinely to perform impact testing. Therefore it has become essential that the instrumentation capabilities in these aeroballistic ranges be expanded to meet test requirements. During Fiscal Year 1979, programs improving these capabilities were carried out. This report summarizes that research.

A sequential laser photography system, initially used in the 100-ft Hyperballistic Range (K)* (Refs. 1 and 2), was adapted to make a five-frame sequence of backlighted photographs of debris clouds generated by impacts of hypervelocity test models with static targets. Also, flash X-ray shadowgraph systems were used to characterize these debris clouds, and an ultra-high-speed framing camera (Beckman & Whitley Model 192) was used to record self-luminosity associated with the hypervelocity impact.

Visible-light and infrared radiometers are used routinely to measure impact radiation at optical wavelengths. To more fully characterize such electromagnetic radiation, radiometers with operating frequencies of 8.6 and 35 GHz were designed and used to measure the impact radiation at microwave wavelengths. A time-integrated spectrometer was used to further characterize visible-light radiation by providing relative intensity-versus-wavelength information. Specially designed "make-screen" debris detection systems were used to produce trigger signals required by some of the aforementioned photographic and radiation measurement systems.

In the following sections, the various instrumentation systems are discussed, and examples of their applications during hypervelocity impact tests are presented.

*Henceforth called Range K. Range G and Range S1 are the shortened names for the 1,000-ft Hyperballistic Range (G) and the Hypervelocity Impact Range (S1), respectively.

2.0 SEQUENTIAL LASER PHOTOGRAPHY SYSTEM

An innovative sequential laser photography system had been designed and used in Track K* for observing the one-to-one particle-to-test model and particle-to-bow shock encounters (Refs. 1 and 2). This high-speed photographic system, which can be operated at framing rates of up to 10^7 sec^{-1}, provides an excellent means for observing the formation and growth of debris clouds generated by hypervelocity impacts. The optical configuration of this track system was modified for range impact use; the schematic of the system for the Range-K impact studies is shown in Fig. 1. The system consists, basically, of five individual backlight laser photography systems located very close to one another. Images formed by the five systems are separated geometrically (i.e., light from one particular laser enters only one particular lens of the multilens camera). Figure 2a shows the arrangement of the five lasers, and Fig. 2b shows the multilens camera. Specially designed electronics allow varying the time between laser firings (photographic exposures) from 100 nsec to 100 msec. At the minimum between-frames time setting (100 nsec), an effective framing rate of 10^7 sec^{-1} is achieved. The 100-msec duration between frames corresponds to an effective framing rate of 10^4 sec^{-1}. The exposure time per frame is 20 nsec, defined by the pulse duration of the pulsed ruby laser. The photographic optics allow resolution of objects as small as 0.001 in.

Examples of the use of the sequential laser photography system during impact tests in Range K are shown in Fig. 3. Figure 3a depicts the progression of the debris cloud formed by the impact of a small projectile traveling at 15,000 ft/sec on a thin target. Time between frames is 7 msec; this yields an effective framing rate of approximately 143,000 sec^{-1}. Figure 3b shows results representative of those obtained with the sequential photography system during a dual-target test; the debris cloud formed by impact with the first target is shown moving toward, and, in the fifth frame, striking a second target. The test conditions and camera conditions were the same as those for Fig. 3a. The actual target thicknesses cannot be seen in these photographs; the target support frame is silhouetted in these edge-on-views.

Results of an oblique impact with a multitarget arrangement are depicted in Fig. 3c. The debris cloud caused by the impact of a small hypervelocity (10,000 ft/sec) projectile with the first target is shown as it moves toward the second target. As in Figs. 3a and b, the actual target thicknesses are obscured by the silhouettes of the target-holding frames. A 6-μsec,

---

*Range K, track-guided mode of operation.

between-exposure time was used in the five-frame sequence shown in Fig. 3c; this yielded an effective framing rate of approximately 167,000 sec^{-1}.

Data describing the overall velocity and growth characteristics of debris clouds can be obtained from the sequential laser photographs.

3.0 X-RAY SHADOWGRAPH SYSTEMS

Flash X-ray shadowgraph systems have been used for many years in the AEDC-VKF aeroballistic ranges. These high-speed (30-nesc exposure time) photographic systems have been used to record stop-motion shadowgrams (radiograms) of hypervelocity models and sabots (Ref. 3). These shadowgraphs have been recently adapted for observing impact phenomena and, in particular, for detailed characterization of debris clouds. To optimize the photographic quality of the X-ray shadowgrams obtained during these impact studies, investigations of system geometry and of the use of a soft X-ray source were conducted.

For minimum penumbral blur (maximum photographic quality) in the shadowgram, the X-ray source size and the object-to-film distance should be minimal and the source-to-object distance should be maximal (Ref. 4). The source size is essentially fixed for the particular X-ray tube in use, and the source-to-object distance that may be used is determined largely by the physical size of the range and by the geometry of the target installation inside the range. Also, the reduced penetrative capability of the X-rays that accompanies attempts to maximize source-to-object distance must be considered. An attempt was made to minimize the object-to-film distance commensurate with an acceptably low chance of film damage during the impact tests. A thin metallic cover protected the X-ray film from the impact debris. An object-to-film distance of only 13.75 in. was used. Figure 4 shows, schematically, the X-ray shadowgraph system used in range impact tests.

Using the arrangement shown in Fig. 4 (with a Hewlett-Packard Model 2722, 180-kv source), experiments were conducted to determine the minimum sizes of aluminum and steel objects that could be discerned in the shadowgrams. Aluminum and steel spheres ranging in size from 1/64 to 1/8 in. in diameter were photographed with an X-ray shadowgraph system. It was concluded that, for the spheres to be discernible in the shadowgrams, the aluminum and steel spheres had to be 1/16 and 1/32 in., respectively, in diameter.

Use of soft X-rays (low-voltage) provides a means to obtain high photographic quality (high contrast) in low object density regions at the expense of penetration capability. A soft

X-ray system using a Hewlett-Packard Model 130-5335-00 tube was evaluated during the Range-K impact tests, but the system was judged impractical because of the hostile environment into which the film had to be placed. The film could not be protected by a thin metallic cover—the protection used with the hard X-ray (high voltage) system—because the soft X-rays would have been completely absorbed by the metallic cover. Consequently, much of the information in the soft X-ray shadowgram was obliterated physically by the impact debris.

X-ray shadowgrams of an impact debris cloud are shown in Fig. 5. These examples were recorded during the same Range-K shot as was the five-frame sequence of photographs in Fig. 3c. The Fig. 5 examples were obtained with hard X-rays (Hewlett-Packard Model 2722, 180-kv system). The X-ray shadowgraph system that recorded the shadowgram of Fig. 5a is located just downrange of the second target plate; the debris cloud shown is the result of impact of the debris cloud shown in Fig. 3c with the second target plate. Some of the downrange side of the second target plate can be seen in Fig. 5a. The shadowgram in Fig. 5b was recorded approximately 1 ft farther downrange than was that of Fig. 5a; Fig. 5b depicts the debris cloud just before it impacts a third target plate. A third X-ray shadowgraph system is often used to record the debris resulting from impacts with the third target plate.

Data describing debris velocity and mass are obtained from the X-ray shadowgrams. Information concerning the distribution of the debris (particle) mass and velocity may be derived from these shadowgrams.

4.0 HIGH-SPEED FRAMING CAMERA

A Beckman & Whitley Model 192 high-speed framing camera has been used in Range S1 for sequential observations of the luminosity generated by hypervelocity impacts. Such observations have allowed detailed studies of the relative intensity, physical extent, and growth rate of the luminous region occurring on the launcher side of the first target upon impact by a projectile.

The Beckman & Whitley camera can record 80 frames at a maximum framing rate of 1.4×10^6 sec^{-1}. Figure 6 is a simplified diagram of the camera installation for impact studies. (In the actual installation, four front-surface mirrors are required to fold and direct an optical path from the camera to the target area.) The distance from the camera lens to the target (impact point) was 25 ft.

Figure 7 shows a 10-frame sequence of photographs of an impact flash. This flash was produced by the impact of a small projectile at 22,500 ft/sec. The camera framing rate was

1,160,000 sec^{-1}. The time between frames was 860 nsec, and the exposure time per frame was 215 nsec. Thus, this entire sequence of pictures was recorded in less than 8 μsec.

5.0 MICROWAVE RADIOMETERS

Microwave radiometers operating at 8.6 and 35 GHz were used to monitor radiation during impact tests in Range S1. The 8.6-GHz microwave installation scheme is diagrammed in Fig. 8; the same scheme was used for the 35-GHz radiometer. The horn-lens antenna assembly was situated to "view" the initial impact with the first target plate; antenna-to-target distance was one meter.

The microwave radiometers were calibrated with an argon gas discharge tube as a standard white-noise source. Throughout the bandwidths of the microwave receivers, the gas discharge generates white noise that exceeds thermal noise by 16 db $\pm$ 0.5 db.

Data were recorded with the 8.6-GHz system during some shots, but there was no detectable radiation at 35 GHz. The 8.6-GHz radiation data recorded during five shots in Range S1 are plotted in Fig. 9. Radiation values as low as 10^{-14} w/sr-μm were recorded; the maximum recorded value was approximately 3 x 10^{-13} w/sr-μm.

The low-level, 8.6-GHz radiation (Fig. 9) persisted for far longer periods of time (up to 700 μsec) than can be attributed directly to energy release upon impact. For comparison, radiation recorded by visible-band radiometers observing these same events in Range S1 lasted for time periods only of about 2 μsec; the magnitude of spectral radiant intensity recorded by the visible-band radiometers was about 25 kw/sr-μm. One possible explanation for the long-duration, low-intensity, 8.6-GHz radiation is that upon impact, a plasma is generated with effective electron density levels at or above the critical density (Ref. 5) associated with 8.6-GHz radiation (9.2 x 10^{11} cm^{-3}); because of the very low ($\sim$ 1 μm-Hg) ambient pressure, the recombination (free electrons recombining with ions) is relatively slow, thus producing observable 8.6-GHz radiation lasting for hundreds of microseconds. The lack of detectable 35-GHz radiation could be explained by the level of plasma ionization: A considerably higher level of plasma ionization would be required to produce 35-GHz radiation than to produce 8.6-GHz radiation. The critical electron density associated with 8.6-GHz radiation is 9.2 x 10^{11} cm^{-3} (as mentioned above), whereas the critical density associated with 35-GHz radiation is 1.52 x 10^{13} cm^{-3} (Ref. 5). Visible radiation from the recombination process would not be expected to reach the detection threshold of the visible-band radiometers, which are set to record extremely high-intensity radiation.

6.0 TIME-INTEGRATED SPECTROMETER

A time-integrated spectrometer was constructed and used in Range S1 for spectral characterization of impact flashes. (The spectrometer uses a 600 line/mm grating and has a dispersion of 100 Å/mm. Spectral resolution is estimated to be ±30 Å.) This instrument was used to view the first target plate as shown in Fig. 8. The spectrometer was operated in an "open-shutter" mode. The spectra recorded were time integrated over the entire multiple-target impact process; it is likely that some light from impacts with the second and third targets reached the spectrometer through and around intervening targets.

Spectra are recorded on photographic film. The spectrometer is not calibrated for absolute intensity measurement but is wavelength calibrated using a mercury vapor light source. A densitometer is used to read photographic density of spectral lines on the film. A computer program that takes film response characteristics into account transforms film density values into relative intensities. Figure 10 shows an example of the reduced spectral data from an impact flash. The somewhat abrupt cutoffs near 4200 and 6400 Å result from reaching the bandpass limits of the spectrometer. This approximately 2200-Å-wide bandpass can be shifted as desired within a 3500- to 6800-Å overall-wavelength band.

7.0 MAKE-SCREEN MODEL/DEBRIS DETECTION SYSTEMS

Most impact instrumentation systems, especially photographic systems, require a means for precisely detecting the arrival of a model or debris cloud at a particular measurement station; a properly timed trigger pulse must be provided to activate the instrumentation system. It was not practical to use optical barrier techniques (e.g., continuous-wave laser/photodiode technique described in Ref. 2) for model detection because of field-of-view limitations and physical constraints. Thus, special make-screen model/debris detection systems were designed to provide trigger signals required by many of the photographic and radiation measurement systems used for this work.

A photograph of a make-screen device used for model detection is shown in Fig. 11a. This make-screen is approximately 3 by 4 in. Make-screens used for detection of debris clouds must, of course, be somewhat larger, some as large as 14 by 24 in. Also, make-screens for debris detection must be mounted in such a manner that the holding device does not interfere with the impact experiment and does not obstruct view if the device being triggered is a photographic system.

The make-screen detector consists of a sheet of metalized Mylar® and a circuit (Fig. 11b) connected through a length of two-conductor cable. The make-screen detector is made from

special, 0.001-in.-thick Mylar that has a thin (nominally 0.0005-in.-thick) deposit of aluminum on both sides. The electronic circuitry used with a make-screen is shown in Fig. 11b. Capacitor C1 is charged to 150 v. As a model or debris particle penetrates the make-screen, the two aluminum surfaces are shorted. This electrical short provides a discharge path for capacitor C1 through capacitor C2 and resistor R3, thus developing a positive voltage pulse across R3. This pulse can be appropriately conditioned and delayed with additional electronic circuitry and used as a trigger signal.

The make-screen detection scheme has been used extensively during recent impact tests in Ranges G, K, and S1 for triggering both model and debris X-ray shadowgraph systems. Faint images of make-screens can be seen in the X-ray shadowgrams of Fig. 5. The make-screens shown in Fig. 5 are the ones that initiated trigger pulses for the two X-ray shadowgraph systems.

Make-screen detection systems have shown a high degree of reliability for properly triggering X-ray shadowgraphs. During the recent impact tests in Ranges G, K, and S1, shadowgrams of hypervelocity models were recorded for 166 of the possible 190 occasions, thus giving 87 percent reliability. As expected, reliability for debris detection was slightly lower; properly timed shadowgrams were obtained on 26 of 33 occasions, or 79 percent of the time. It should be noted that none of the failures to trigger could be attributed to failure of the make-screen to electrically short. Most triggering problems resulted from such events as cross talk with other systems, improperly chosen delay times, and malfunctions of peripheral electronics (pulse amplifiers/conditioners).

8.0 CONCLUDING REMARKS

The instrumentation capabilities of the AEDC-VKF aeroballistic ranges have been expanded significantly for impact testing by developing and implementing the instrumentation systems described herein. Detailed studies of the dynamic results of hypervelocity impacts are now possible: The extremely high-speed sequential laser photography system provides data describing the overall velocity and growth characteristics of debris clouds. X-ray shadowgraph systems yield data describing debris velocity and mass, and information concerning mass (particle) distribution and individual particle velocity.

Electromagnetic radiation generated by hypervelocity impact can now be explored in several ways: The high-speed framing camera allows studies of the relative intensity, physical extent, and growth and decay rates of impact flashes. The development of microwave radiometers makes possible the quantitative measurement of radiation associated with hypervelocity impact at two frequencies in the centimeter-wave region of the

electromagnetic spectrum—8.6 and 35 GHz. The time-integrated spectrometer provides data characterizing the impact flash in terms of relative intensity versus wavelength. Make-screen detection systems provide reliable trigger signals for both old and new photographic and radiation measurement systems.

REFERENCES

1. Dugger, P. H. "Aeroballistic Range/Track Photographic Instrumentation Development." AEDC-TR-77-98 (AD-A053591), April 1978.

2. Hendrix, R. E. and Dugger, P. H. "Photographic Instrumentation in the VKF Aeroballistic Track Facilities." In *Proceedings*, 13th International Congress on High-Speed Photography and Photonics, Tokyo, Japan, 1978. Society of Photo-Optical Instrumentation Engineers, Bellingham, Washington, 1979.

3. Hendrix, R. E. and Dugger, P. H. "High-Speed Photography in the Aeroballistic Range and Track Facilities of the von Kármán Gas Dynamics Facility." In *Proceedings,* 12th International Congress on High-Speed Photography, Toronto, Canada, August 1—7, 1976. Richardson, Martin C., ed. Society of Photo-Optical Instrumentation Engineers, Bellingham, Washington, 1977.

4. Henderson, W. F., Robertson, G. W., Jr., and Hill, J. W. "Investigation of Shadowgraphs for use with Highly Ablating Self-Luminous Ballistic Projectiles." AEDC-TR-71-225 (AD734742), December 1971.

5. Hendrix, R. E. "Radio Frequency and Microwave Flow-Field Diagnostic Techniques in Aeroballistic Ranges—A Comprehensive Survey." AEDC-TR-69-215 (AD867943), April 1970.

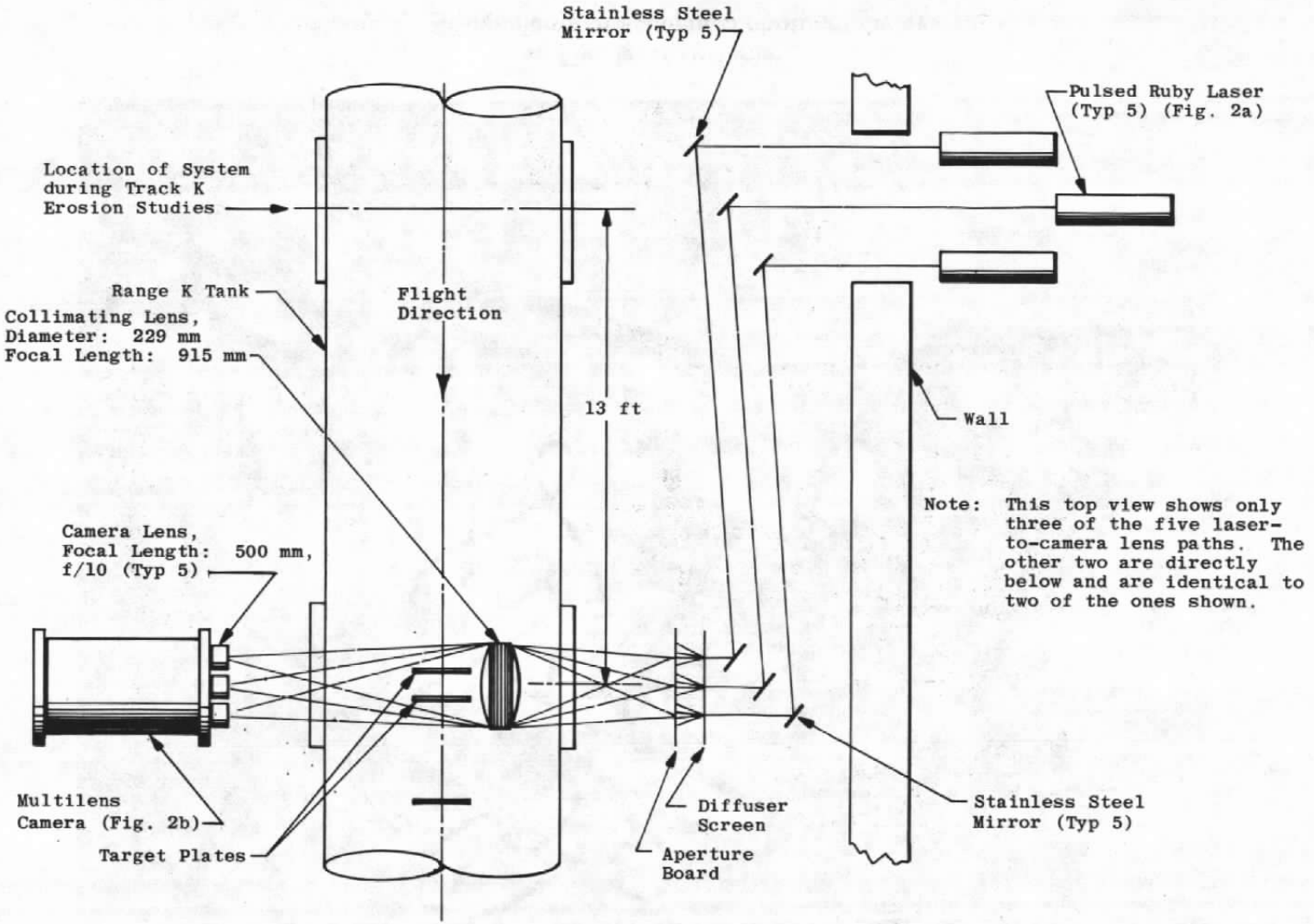

Figure 1. Sequential laser photography system installation

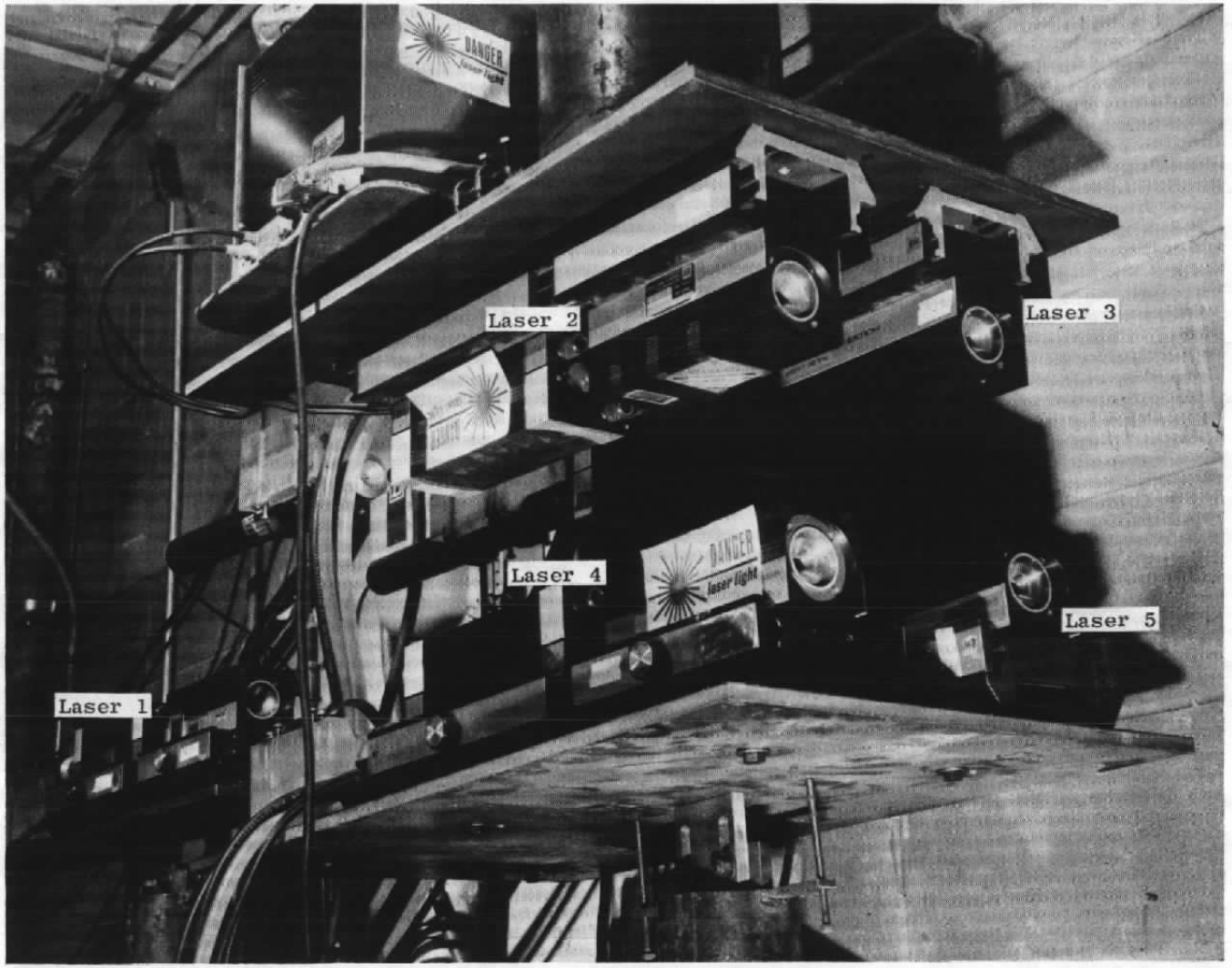

a. Five laser systems

Figure 2. Components of sequential photography system

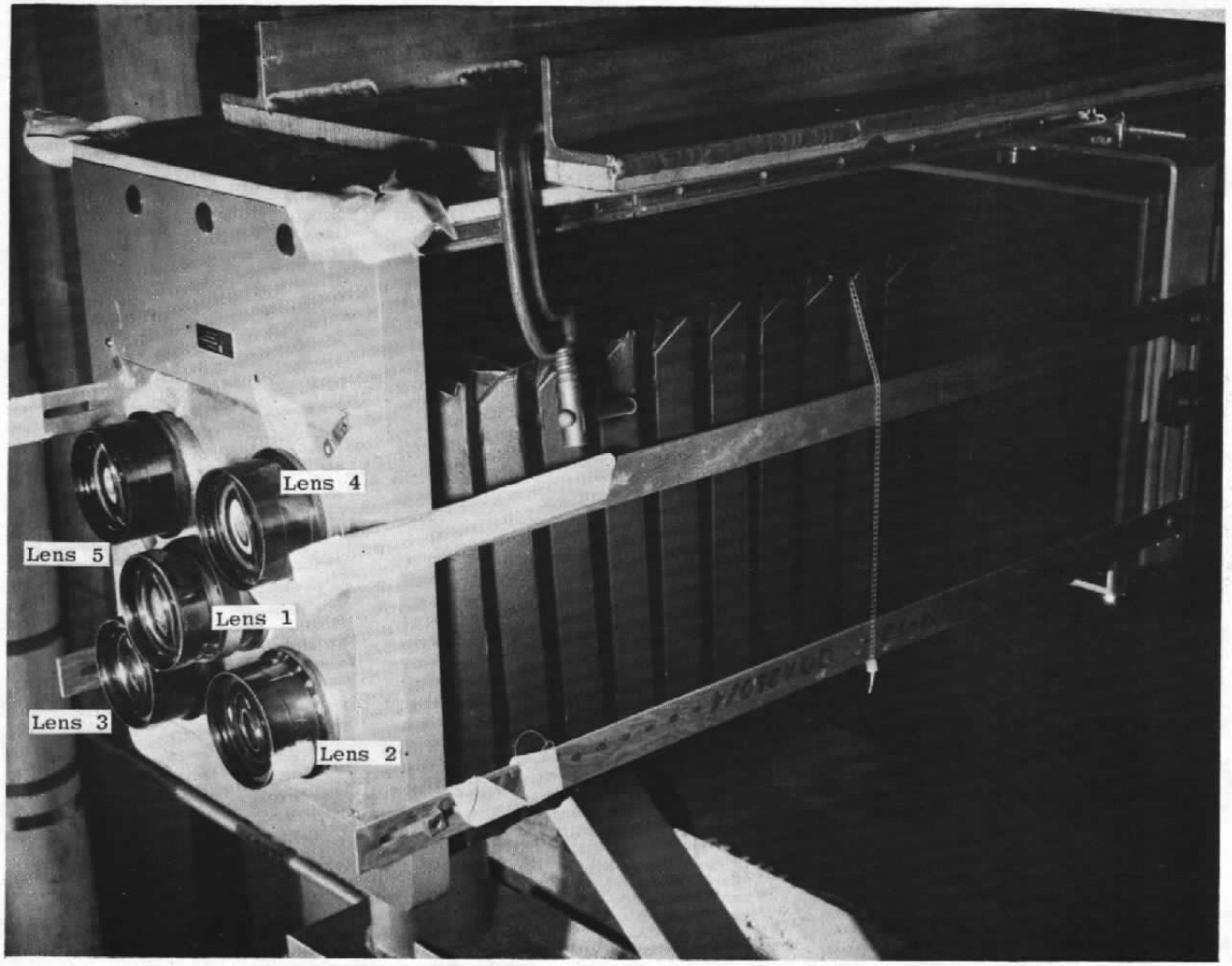

b. Multilens camera
Figure 2. Concluded.

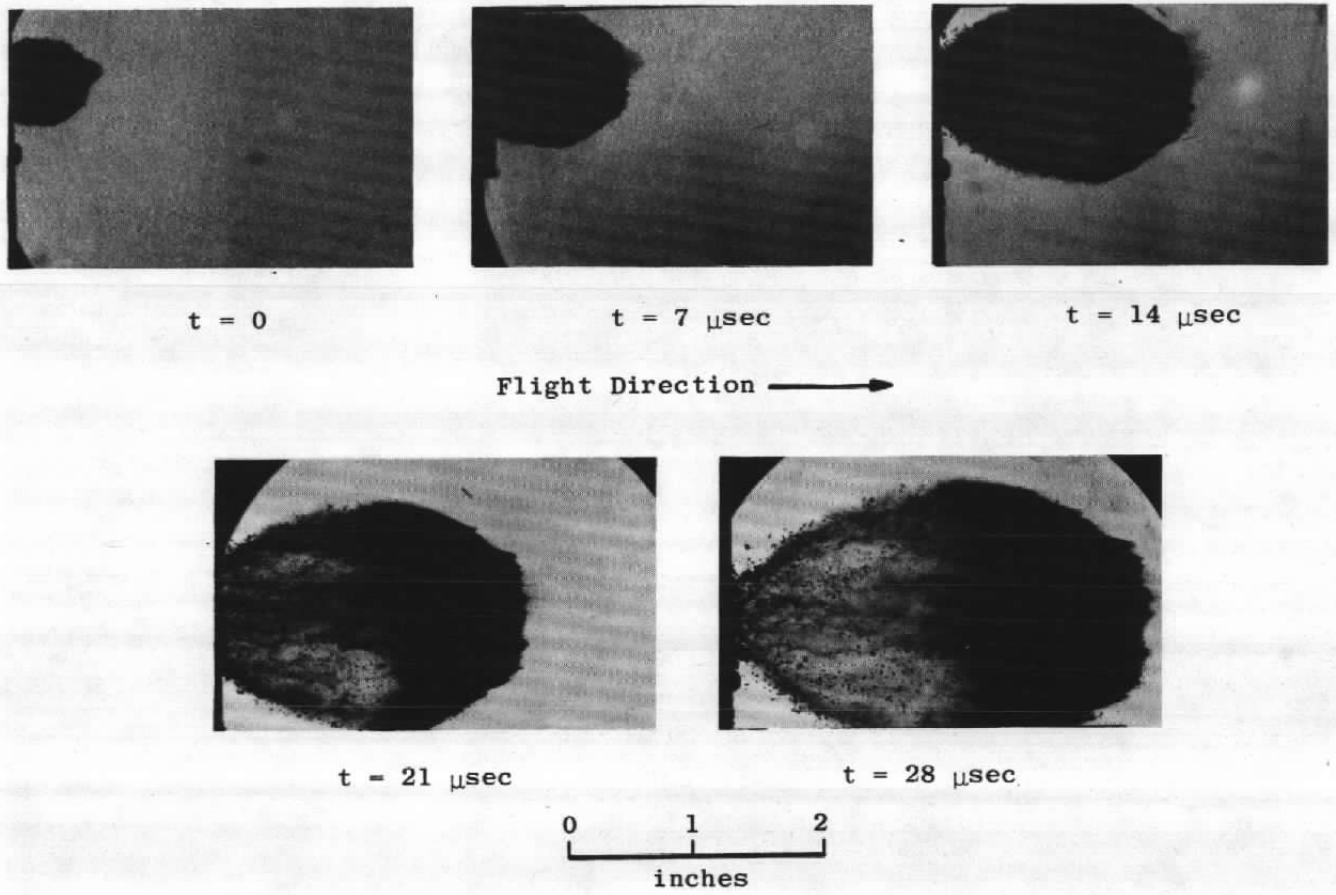

a. Single vertical target

Figure 3. Sequential laser photographs depicting impact debris

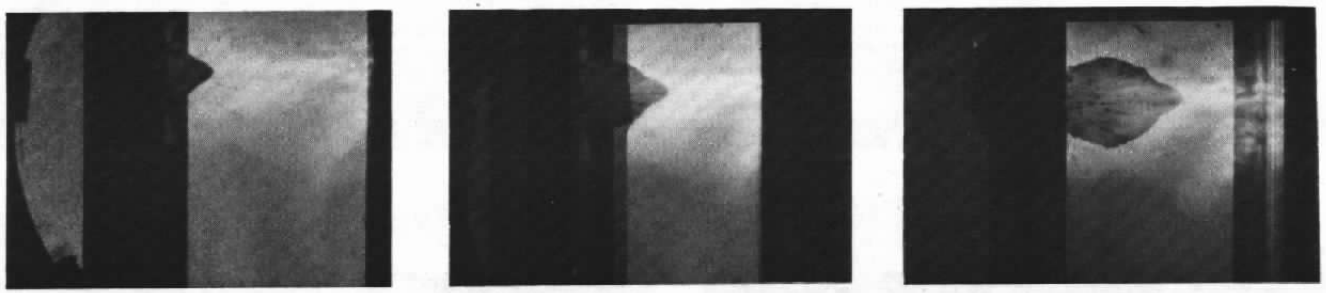

b. Double vertical target
Figure 3. Continued.

t = 0 t = 6 μsec t = 12 μsec

Flight Direction ⟶

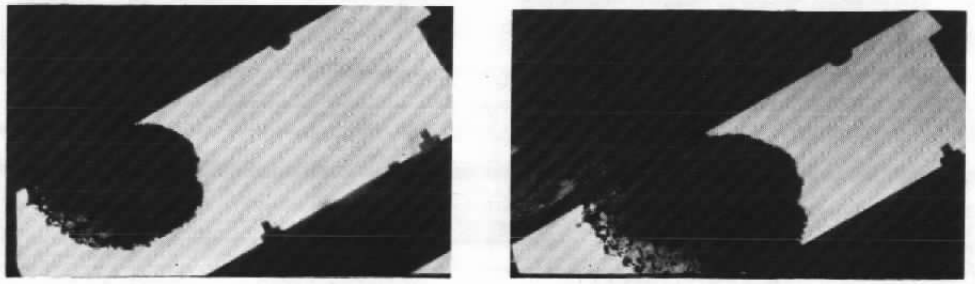

t = 18 μsec t = 24 μsec

0 1 2
inches

c. Oblique targets
Figure 3. Concluded.

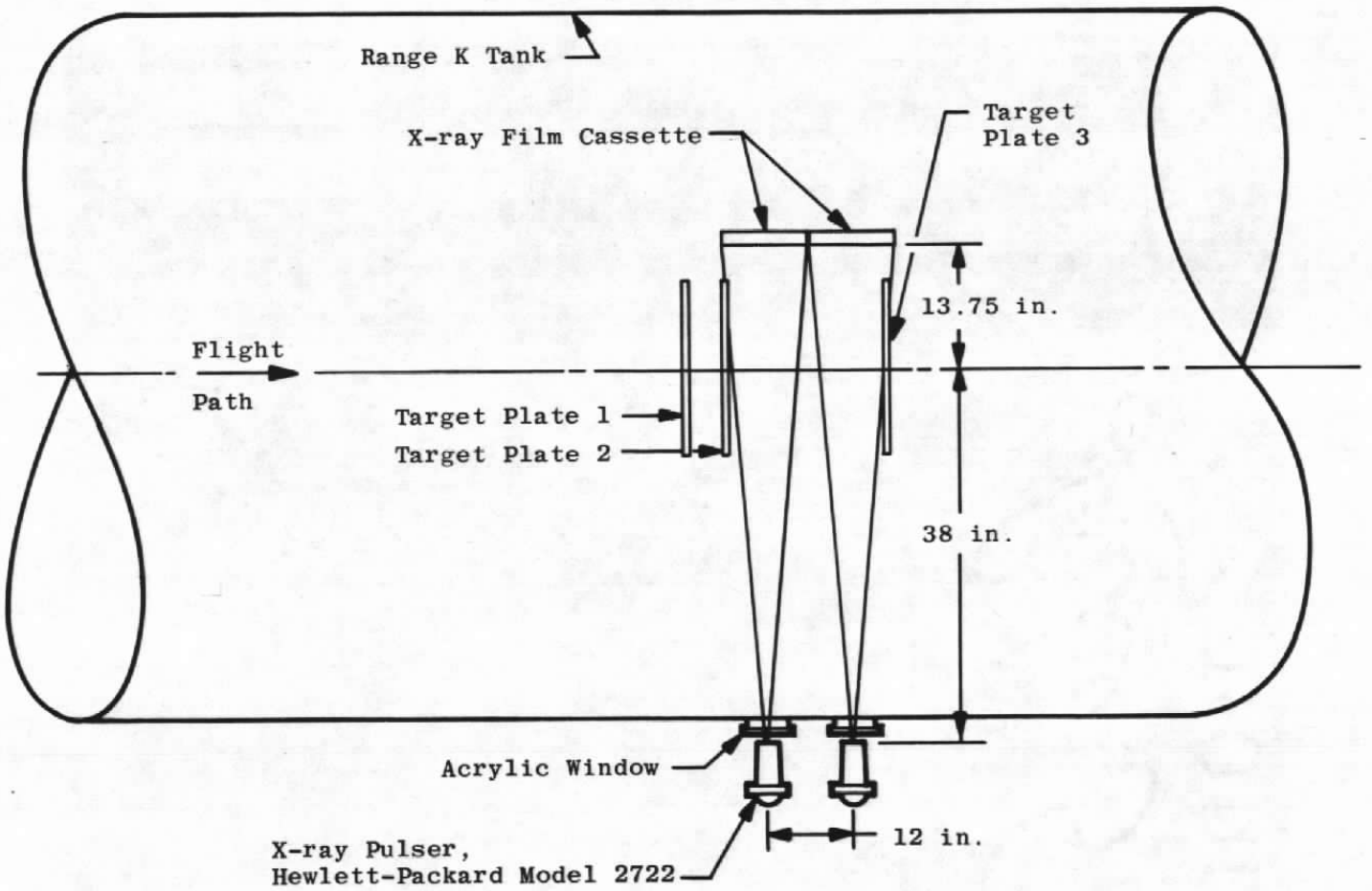

Figure 4. X-ray shadowgraphs for debris observation.

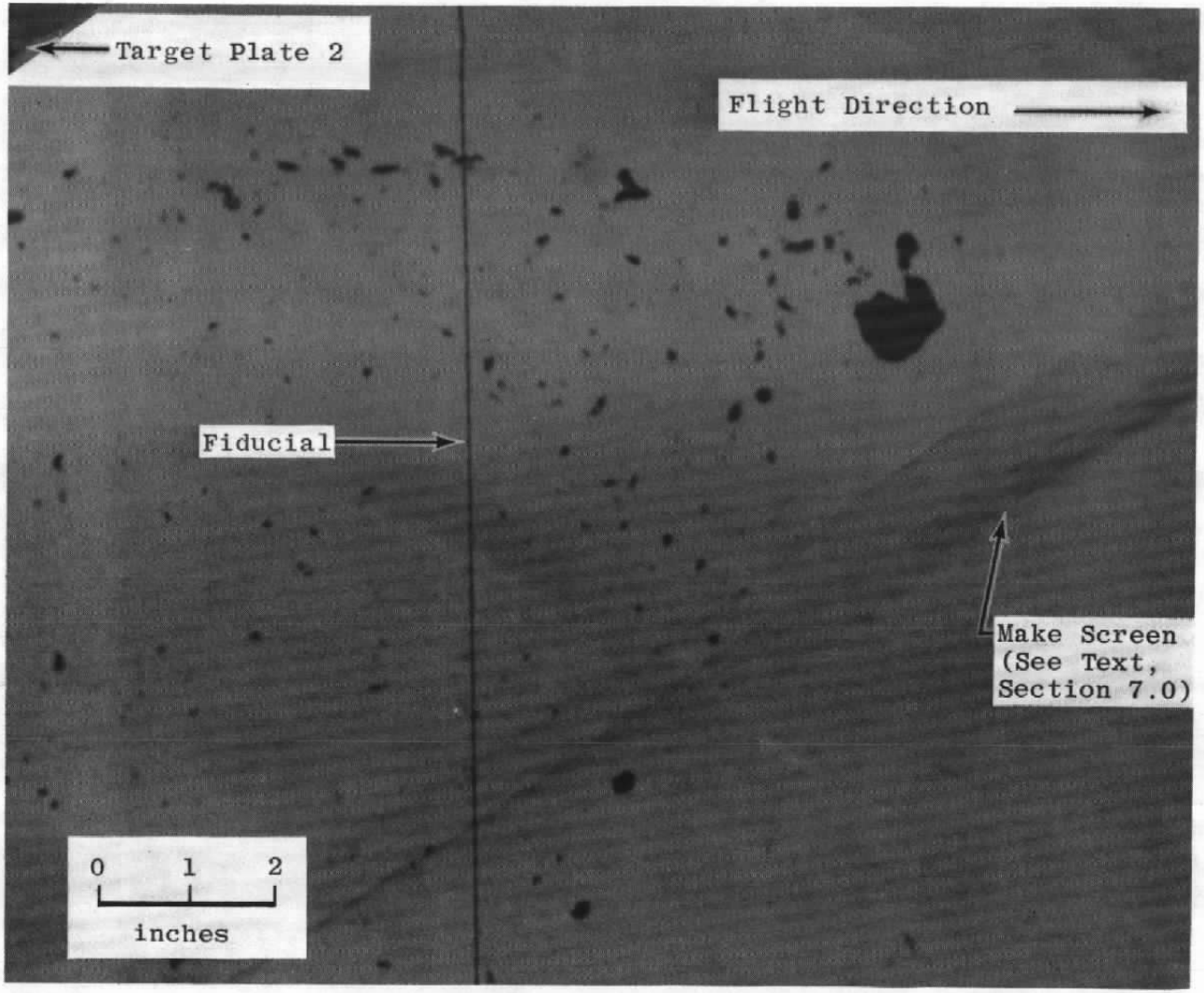

a. After second target plate

Figure 5. X-ray shadowgrams of impact debris.

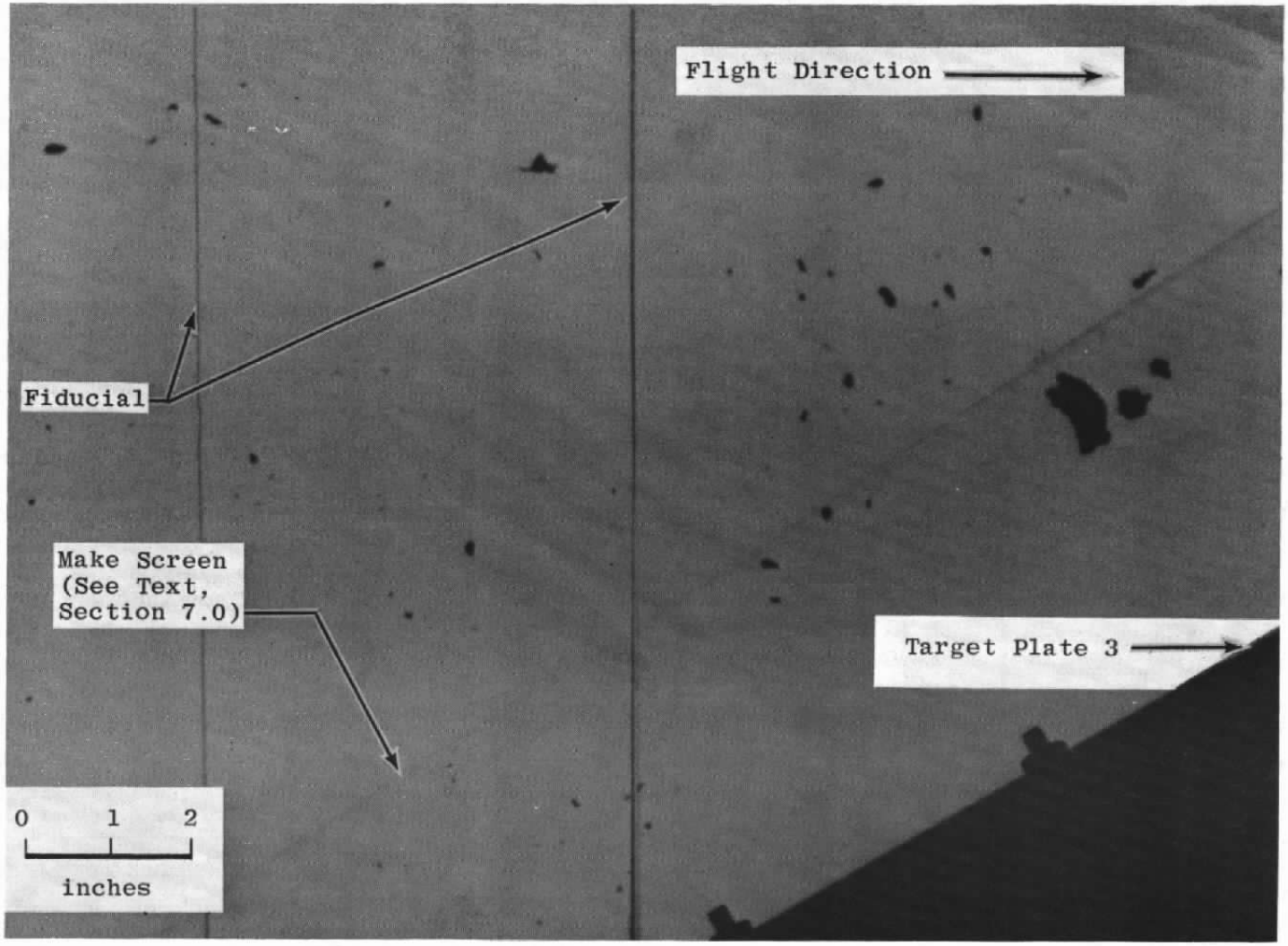

b. Just prior to third target plate
Figure 5. Concluded.

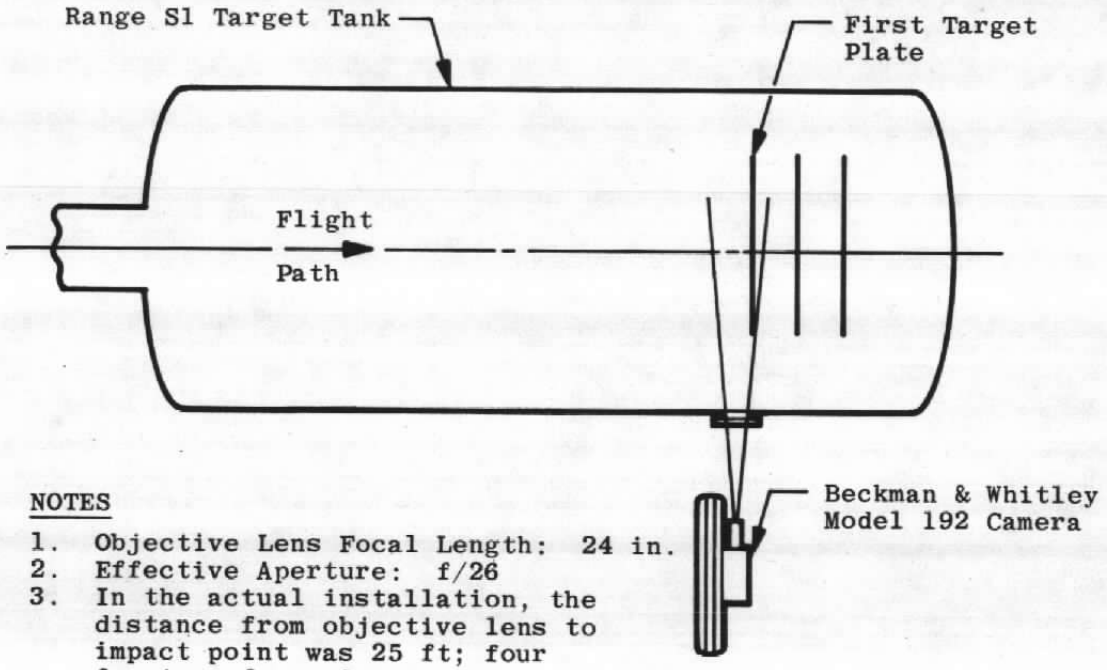

NOTES

1. Objective Lens Focal Length: 24 in.
2. Effective Aperture: f/26
3. In the actual installation, the distance from objective lens to impact point was 25 ft; four front-surface mirrors were included in this optical path.
4. Magnification: ~0.1

Figure 6. High-speed framing camera installation (simplified).

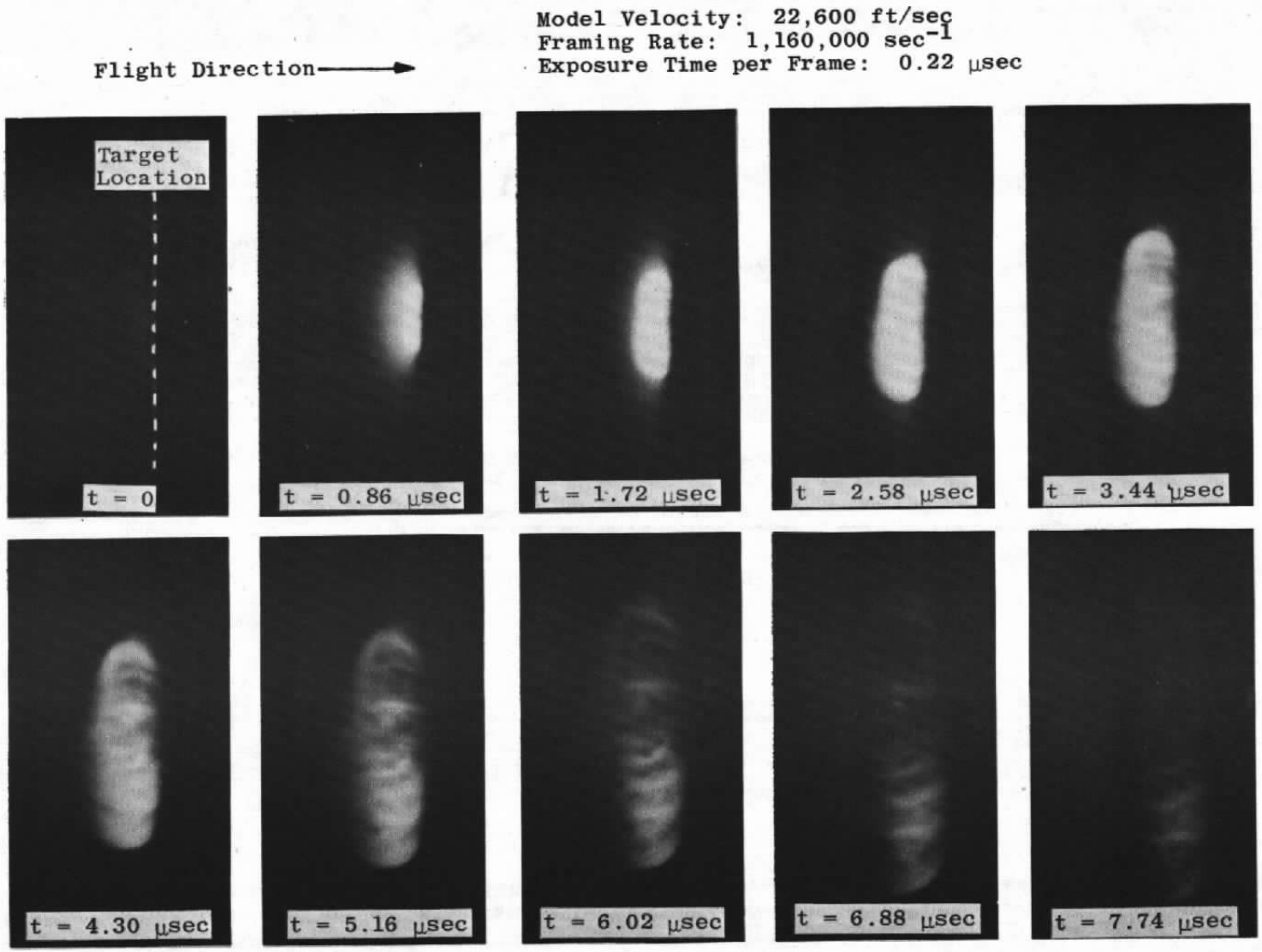

Figure 7. High-speed framing camera photographs of impact flash.

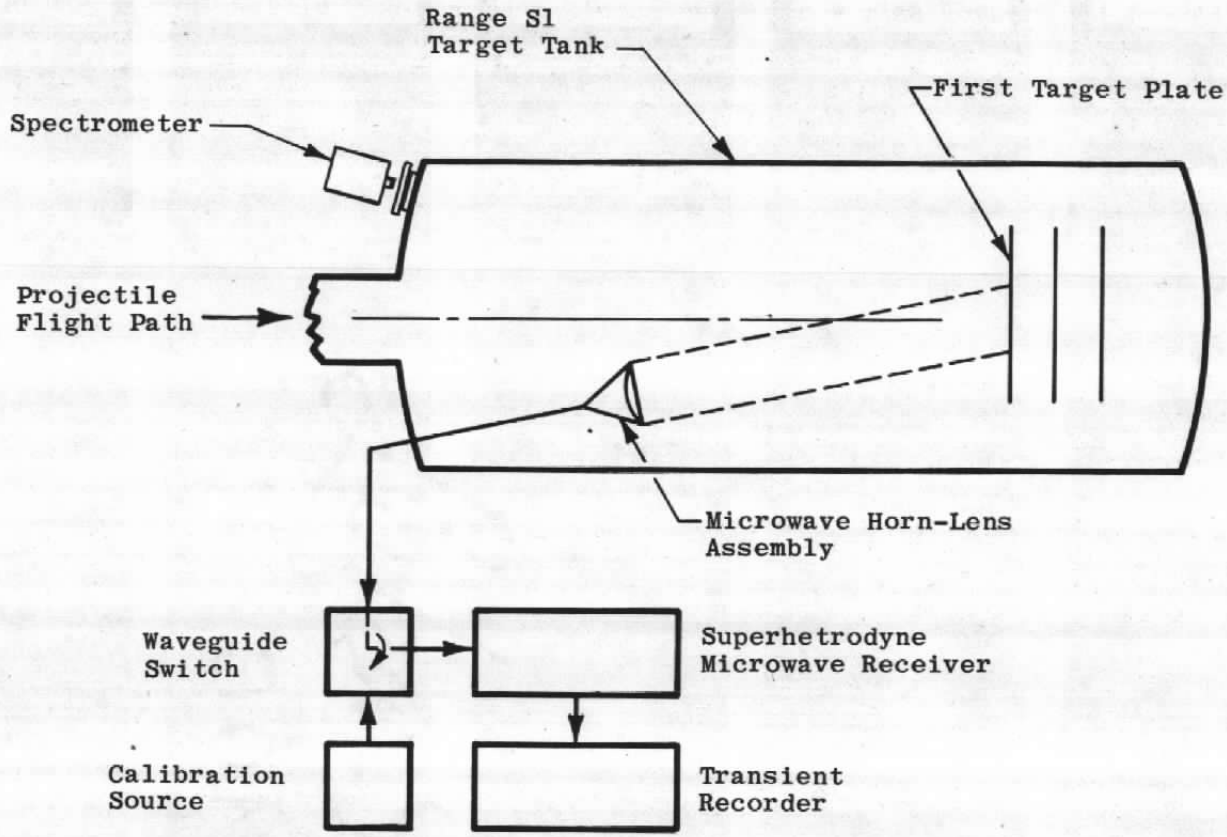

Figure 8. Microwave radiometer and spectrometer installation.

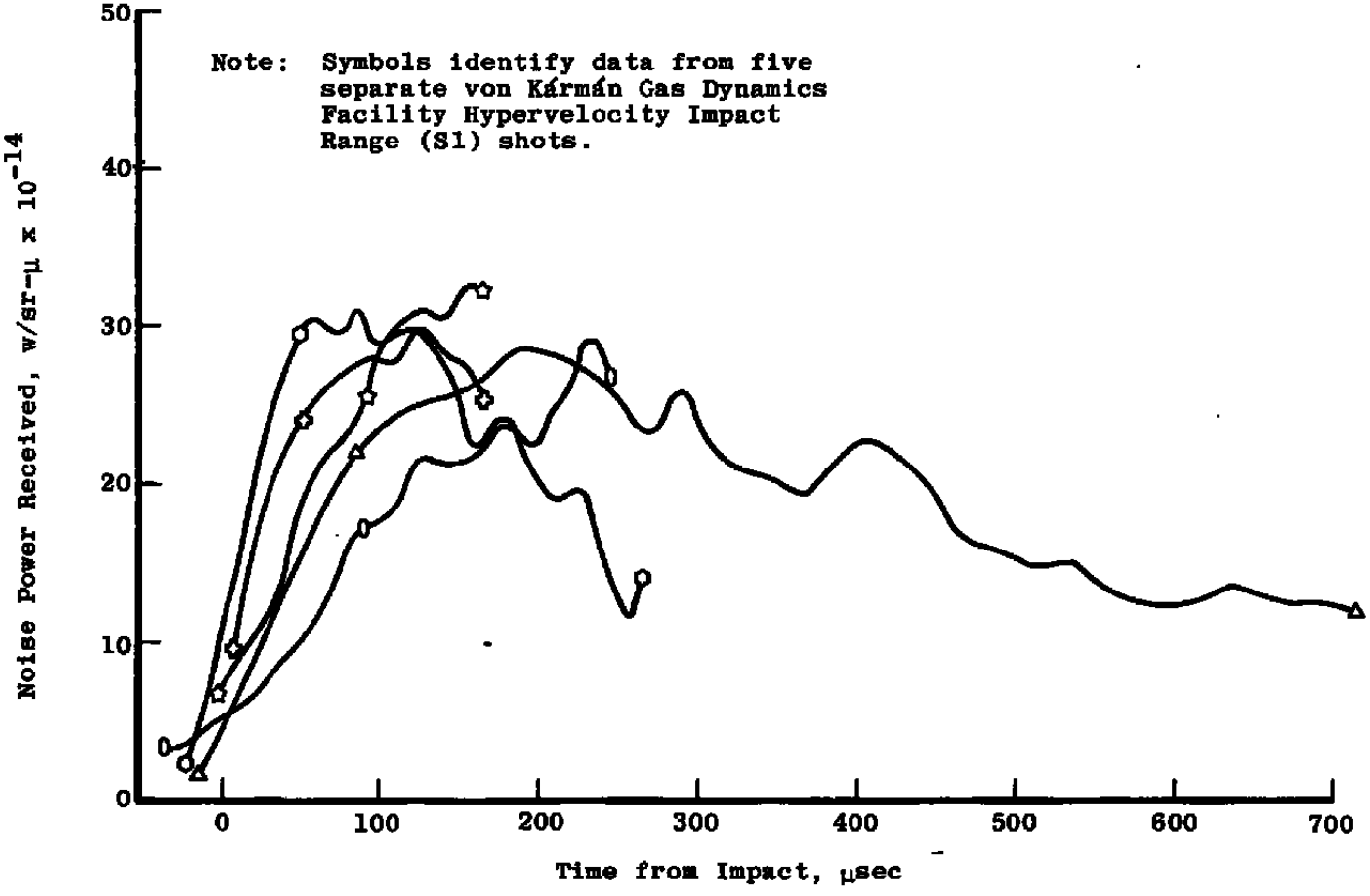

Figure 9. 8.6-GHz radiometer data.

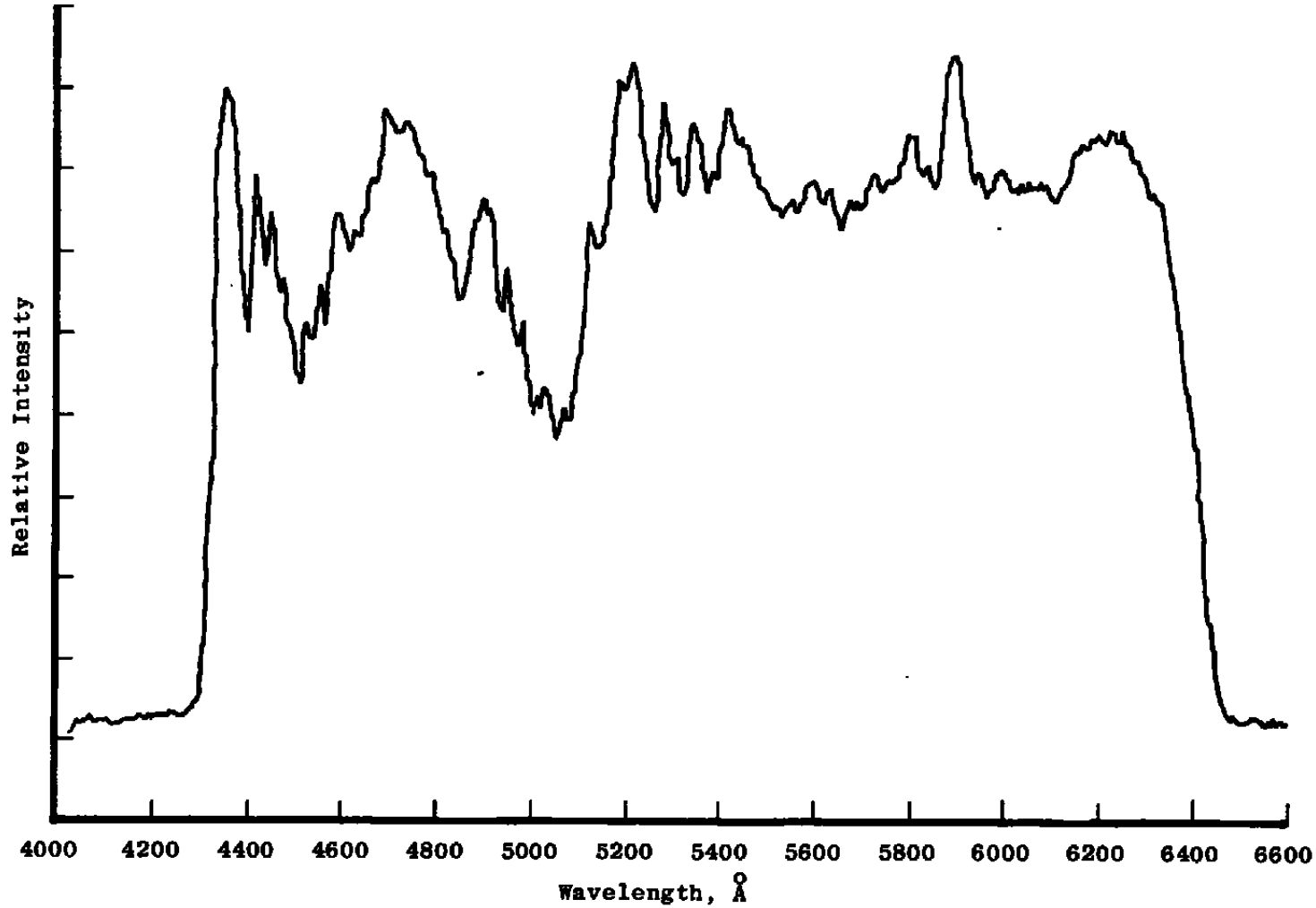

Figure 10. Time-integrated spectrometer data describing impact flash.

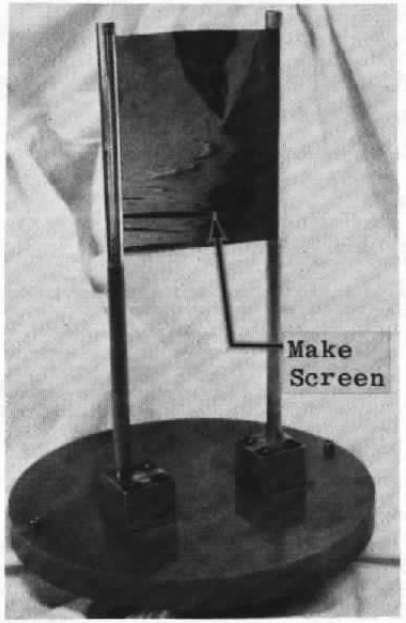

a. Make-screen assembly

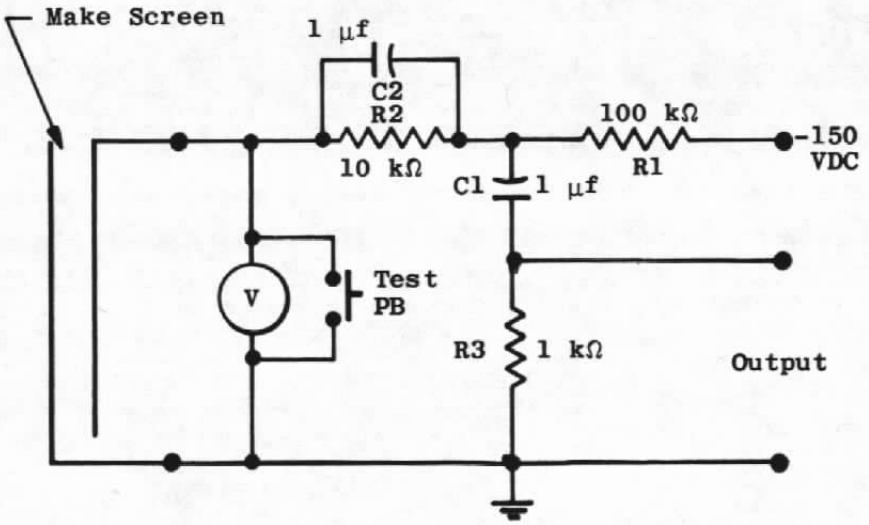

b. Make-screen circuit

Figure 11. Make-screen detection system.